Vibrational and magnetic properties of nano-sized $CoFe_2O_4$ obtained by various synthesis techniques: a comparative study

Z. LAZAREVIĆ[1,*], Lj. ANDJELKOVIĆ[2], M. ŠULJAGIĆ[2], A. MILUTINOVIĆ[1], M. ĆURČIĆ[1], J. TRAJIĆ[1], N. PAUNOVIĆ[1], M. ROMČEVIĆ[1], B. HADŽIĆ[1], N. ROMČEVIĆ[1]
[1]*Institute of Physics Belgrade, University of Belgrade, 11080, Belgrade, Serbia*
[2]*University of Belgrade, Institute of Chemistry, Technology and Metallurgy, Department of Chemistry, 11000 Belgrade, Serbia*

Nanocrystalline $CoFe_2O_4$ has been synthesized by various synthesis methods. The obtained monodomain nanoparticles are similar in sizes (15.8-19 nm), but with different internal stresses, size distributions and cation inversion coefficients (0.51 - 0.90) due to different synthesis routes. The structure and cation distribution are investigated by XRD diffraction analysis, Raman and FIR spectroscopy. Measurement of magnetization, i.e. coercivity, enable the calculation of the anisotropy coefficient $K_1 = (3.6\text{-}5.12)\cdot 10^5$ J cm^{-3}, which is very high in cobalt ferrite. The anisotropy coefficient directly depends on the nanoparticle size. It has been shown that magnetization linearly depends on the cation inversion, except in the sample with the largest nanoparticles (19 nm), where the more regular crystal structure prevails and higher values of magnetization were obtained. The average magnetic moments at 300 K are: $\mu_{Fe} = 3.6\mu_B$ and $\mu_{Co} = 2.5\mu_B$. It is obvious that with small adjustments in the synthesis, desirable nanoparticle properties can be obtained.

(Received December 6, 2022; accepted June 6, 2023)

Keywords: $CoFe_2O_4$, XRD, Raman, Far-infrared spectroscopy, Magnetic measurements

1. Introduction

Nowadays, the nanostructured materials are widely used for frontier research areas because of their good physicochemical characteristics which are not shown by many material of similar compositions in their bulk counterpart [1, 2]. Among the many nanomaterials, transition type metal oxide based materials are gaining more attention by researchers due to a wide range of broad spectrum of applications such as medical, energy storage, fabrication of advanced devices, etc.

A lot of synthetic strategies for preparing nanosized cobalt ferrite in diameter of 2-50 nm have been presented [3]. However, their application can be limited due to the surfactants that are covered on the surface of the ferrite particles and hard to be removed.

Spinel ferrites (MFe_2O_4) have attracted considerable attention over the past years. The structural, optical, magnetic, and mechanical properties of these ferrites allow their successful application in various areas, such as electronic devices and the biomedical field [4]. Spinel ferrite nanoparticles are currently some of the most important and versatile advanced ceramics. Several works show that this easy processing material brings technological innovation in gas sensors, catalysts, microwave-absorbing materials, permanent magnets, high-density recording media and magnetic hyperthermia applications [5].

Cobalt ferrite ($CoFe_2O_4$) is a spinel ferrite with a large coercive field compared to the other soft ferrites. It is considered as a semi-hard material due to its coercive field value located between the soft and the hard aspects. Cobalt ferrite still captures the interest of the scientific community by dint of its several characteristics such as large coercivity, moderate saturation magnetization, good chemical stability [6].

In this work, the effect of synthesis method (US-CO ultrasonically assisted coprecipitation, CO - coprecipitation, MC-CO coprecipitation followed by mechanochemical treatment, MW-HT microwave assisted hydrothermal method and ME microemulsion method) on the structural, vibration and magnetic properties of cobalt ferrite were investigated. The primary aim of this work is to eliminate the using of expensive dangerous chemicals in preparing ferrite magnetic materials and instead using cheap, simple and environmental friendly materials.

The second aim is to characterize the entire prepared nanosized partially inversed cobalt ferrites, $(Co_{1-x}Fe_x)^A[Fe_{2-x}Co_x]^B$, using different techniques viz. XRD, Raman, far-IR and magnetic measurements in order to obtain information about the impact of the preparation route on the formation conditions, crystal size, cation distribution as well as the morphology of the prepared samples. To the best of our knowledge, no such complete investigations for $CoFe_2O_4$ prepared via the entire routes are reported in the literature. The obtained structural,

vibrational and magnetic parameters obtained using different methods will be compared and discussed.

2. Methods and materials

The five synthetic methods, i.e., coprecipitation (CO), mechanochemical (MC), ultrasonically assisted coprecipitation (US-CO), microemulsion (ME), and microwaveassisted hydrothermal (MW-HT) syntheses were chosen for preparation $CoFe_2O_4$ samples. The synthesis procedure is described in detail [7]. The following chemicals were used for the synthesis: iron (III) chloride hexahydrate ($FeCl_3{\cdot}6H_2O$, 98 %), cobalt (II) chloride hexahydrate ($CoCl_2{\cdot}6H_2O$, 98 %), sodium hydroxide (NaOH, >97 %), cetyltrimethylammonium bromide (CTAB, >98 %), n-butanol (99.8 %), n-hexanol (>99 %), iron(III) nitrate nonahydrate (Fe $(NO_3)3{\cdot}9H_2O$, >99.95), cobalt(II) nitrate hexahydrate ($Co(NO_3)_2{\cdot}6H_2O$, >99.99), ammonium hydroxide solution (28 % NH_3 in water), absolute ethanol and soluble starch) were obtained from Sigma-Aldrich (p.a. quality) and used without additional purification. Deionized water was used in these experiments.

Coprecipitation method (CO) is used to obtain $CoFe_2O_4$ powder starting from 0.02 mol Fe^{3+} and 0.01 mol Co^{2+} chlorides as precursors by dissolving them in 50 mL of deionized water and then heating to boiling (a heating rate of 10 $^{\circ}$C min^{-1} at T = 450 $^{\circ}$C for 1 h).

Mechanochemical synthesis (MC) was performed in a planetary ball mill (Retsch PM100CM). A hardened-steel vial (500 cm^3 volume) filled with 10 hardened-steel balls (8 mm in diameter) was used as the milling medium. The powder prepared by the coprecipitation method was ballmilled for 10 h at 500 rpm in closed hardened steel containers with a ball-to-sample mass ratio of 20:1.

Solutions of $CoCl_2{\cdot}6\ H_2O$ and $FeCl_3{\cdot}6\ H_2O$ were mixed in their stoichiometric ratio, during ultrasonically assisted coprecipitation synthesis (US-CO). The concentrations of Fe^{3+} and Co^{2+} were 0.4 M and 0.2 M, respectively. The precipitate was dried at 80 $^{\circ}$C.

The microemulsion (ME) contained 15 wt% hexanol and 45 wt% aqueous solution, and surfactant to cosurfactant ratio was 60/40. Two microemulsions with identical compositions but different aqueous phases were prepared. The first microemulsion contained aqueous solutions of a stoichiometric amount of Fe^{3+} and Co^{2+} nitrates, whereas the second microemulsion contained an aqueous solution of the precipitation agent ammonium hydroxide. These two microemulsions were then mixed under constant stirring and heated for 1 h at 90 $^{\circ}$C.

During microwave-assisted hydrothermal (MW-HT) synthesis used stoichiometric amounts of chloride salts of Fe^{3+} and Co^{2+} necessary to prepare 1.5 g of $CoFe_2O_4$. The mixture was then heated at 200 $^{\circ}$C for 20 min at a maximum pressure of 100 bars.

All produced nanomaterials were thermally treated at 400 °C for 2 h.

XRD patterns were collected using a Rigaku SmartLab automated powder X-ray diffractometer with Cu Kα1 (λ = 1.54059 Å) radiation. The diffraction range was 15-90º with a step of 0.01º at a scan speed of 2º min^{-1}.

The Raman spectra were taken in the backscattering configuration by Jobin Yvon T64000 spectrometer, equipped with nitrogen cooled charged coupled device detector. As an excitation source we used the 532 nm line of Ti:Sapphire laser, with laser power 20 mW. The measurements were performed in the spectrum range 100-1000 cm^{-1}.

The FTIR reflectivity measurements were carried out with a BOMEM DA-8 FIR spectrometer. A deuterated triglycine sulphate (DTGS) pyroelectric detector was used to cover the wave number range from 70-700 cm^{-1}.

Magnetic measurements were performed using a commercial Quantum Design Physical Property Measurement System (PPMS) equipped with a 9 T superconducting magnet and a vibrating sample magnetometer (VSM). Hysteresis loops, M(H), were measured at 300 K in the field range ± 9 T.

3. Results and discussion

3.1. XRD analysis

X-ray diffractograms of five cobalt ferrite samples obtained by various synthesis methods are presented in Fig. 1. It is obvious that all samples are well crystalized in single-phase spinel structure ($Fd\bar{3}m$ space group) with characteristic Bragg reflections indicated in figure in accordance with JCPDS PDF 22-1086. All diffractograms are analysed by means of the *FullProf Suite* (*FPS*) [8]. Achieved Goodness of fit was < 5% for each diffractogram.

To make it easier to see the details of XRD pattern, a small interval of 2θ (from 34-38º), with the reflection (311) and (222), is shown on the left side of Fig. 1. Peaks are practically Lorentzians. There is a noticeable difference in the 2θ positions and broadening of the corresponding reflections in different samples. The auxiliary vertical line coincides with Bragg reflections of the sample with maximal value of 2θ, i.e. smallest lattice constant. Errors in the lattice constants determined by Rietveld refinement of X-diffractograms vary minimally and can be rounded to ±0.0004 Å. The smallest peak width and the biggest nanoparticles has sample ME, synthetized by micro-emulsion method. Estimated average sizes of nanoparticles in samples, obtained by Rietveld refinement, are given with corresponding diffractograms in Fig. 1. The average size (D) and internal strain (e_{str}) of nanoparticles are calculated for all strong peaks in the range 15º-65º 2θ by Williamson-Hall (*W-H*) plot in *Origin Lab*. Data for w_{hkl} (full width at half maximum of a diffraction peaks) and $2\theta_{hkl}$ (peak position) given in *FullProf Suite* "out"-files after refinement are imported in *Origin*. From the intercept ($K{\cdot}\lambda_{Cu}$ / D) and the slope ($4{\cdot}e_{str}$) of the linear function $w_{hkl}{\cdot}\cos\theta_{hkl}$ = f($\sin\theta_{hkl}$):

$$w_{hkl}{\cdot}\cos\theta_{hkl} = K{\cdot}\lambda_{Cu} / D + 4{\cdot}e_{str}{\cdot}\sin\theta_{hkl}$$

the sizes of D with errors from 0.1 to 0.3 nm and the strains e_{str} with error $5 \cdot 10^{-5}$, are estimated.

K is a shape factor (0.94 for mostly spherical particles of cubic symmetry) and λ_{Cu} is a wavelength of used $Cu_{k\alpha 1}$ radiation.

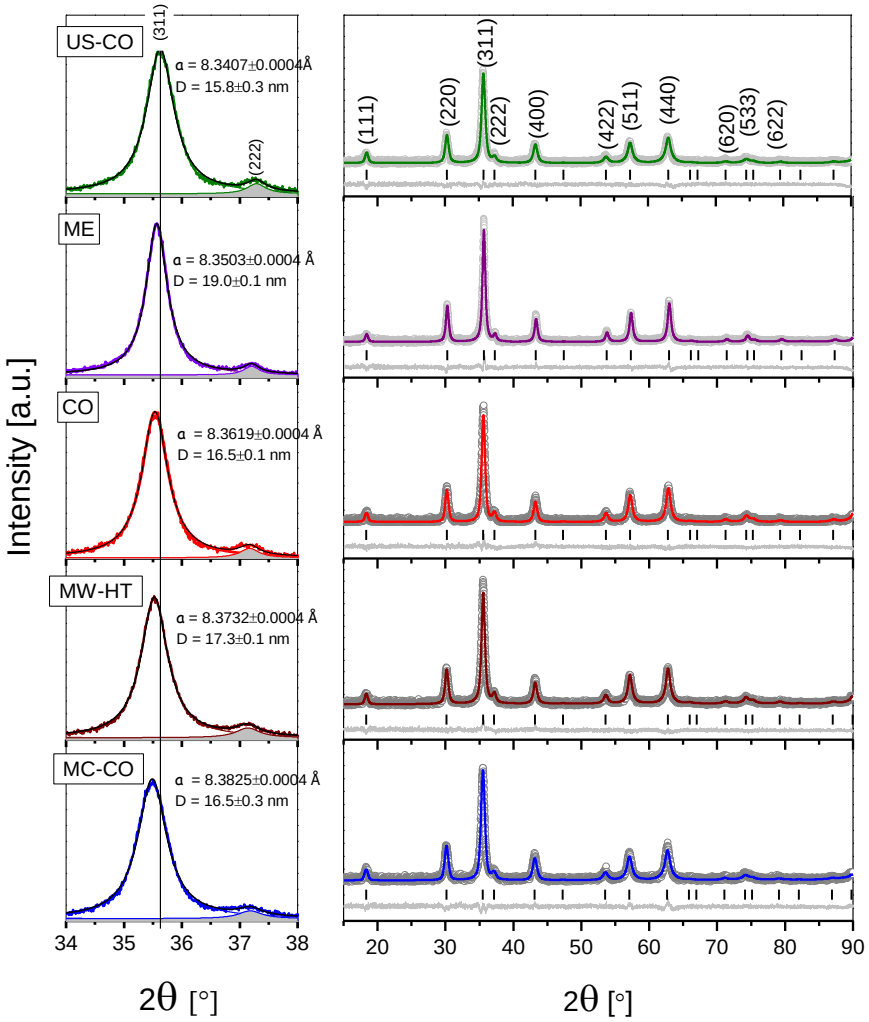

Fig. 1. X-ray diffractograms of cobalt ferrite samples obtained by various synthesis methods, arranged by ascending unit cell parameter a_{exp} - from top to bottom: US-CO - ultrasonically assisted coprecipitation, ME - microemulsion method, CO - coprecipitation, MW-HT - microwave hydrothermal method and MC-CO - coprecipitation followed by mechanochemical treatment. On the left side is shown the part of the diffractograms with the strongest peak (311). The vertical line coincide with the centre of the Bragg reflection of the sample US-CO with the smallest lattice constant (color online)

Obtained values of internal strain are in agreement with known experimental data for cobalt ferrite nanopowders [9, 10]. Smallest strain have samples with bigest nanoparticles ($e_{strME} \approx 6 \cdot 10^{-4}$) and sample CO synthetized by coprecipitation method and the highest values have sample with smallest nanoparticles ($e_{strUS\text{-}CO} \approx 21 \cdot 10^{-4}$) and sample that has undergone mechanochemical treatment (MC-CO). A much more detailed presentation of the results of the XRD-profile and structure analysis will be presented in a separate paper. For this brief report, just one more thing is important: the near-Lorentian profile of the XRD peaks implies a considerable width of the nanoparticle size distribution and the presence of very small nanoparticles in the investigated samples.

The program for the analysis of XRD spectra MAUD, ver. 2.992 [11] gives slightly higher lattice constant values comparing to *FPS*. Both programs are barely sensitive to the inversion of close ^{26}Fe and ^{27}Co cations. MAUD is rather insensitive to the values of oxygen parameters, too. This may be a consequence of a different set of parameters for determining atomic scattering factors compared to *FullProf Suite*. The values of the ionic radii of the cations in MAUD are assumed to be equal in the tetrahedral and octahedral sites – radius of Co^{2+} is 0.65 Å as LS in octahedral coordination, and radius Fe^{3+} = 0.49 Å as HS in tetrahedral site (AtomSite list in "par.lst"-file). In addition, higher values of average nanoparticle size and smaller internal strains are obtained from Rietveld analysis by MAUD comparing to *FPS*. For the sample US-CO, with smallest nanoparticles, MAUD gives a = (8.3451±0.0007) Å, u = 0.3821±0.0004, D = (19.3±0.1) nm and $e_{strUS\text{-}CO}$ = $(17.2 \pm 0.4) \cdot 10^{-4}$. For *ME*, sample with biggest

nanoparticles, is a = (8.3537±0.0005) Å, u = 0.3780±0.0003, D = (25.4±0.2) nm and e_{strME} = (1.7±0.1)·10^{-4}. As we can see, obtained values of a, D and e_{str} don't change their trends, but u behaves less predictably. If we fixed u = 0.375, the parameters of the profile refinement would not be changed.

Based on the lattice constants (a) and oxygen parameters (u) determined via the Rietveld method refinement by *FPS*, a structural analysis of the nano-samples was performed. Using the known relations for the octahedral and/or tetrahedral distances [12], as well as the known Shannon ion radii [13] in the tetrahedral and octahedral sites, the inversion coefficient, x, is estimated for each sample.

$$(R_{tet}=)\ a\sqrt{3}\,(u-1/8)=(r_{Co}{}^{A}(1\text{-}x)+r_{Fe}{}^{A}x)+r_{O}$$

$$(R_{oct}=)\ a\sqrt{3u^2-2u+3/8}=\tfrac{1}{2}\cdot[r_{Fe}{}^{B}(2\text{-}x)+r_{Co}{}^{B}x]+r_{O}$$

The results are shown in Table 1.

Table 1. Lattice parameters (a) and oxygen parameters (u) are obtained by Rietveld analysis. Cation inversion coefficients (x) are estimated from XRD structural analysis. Inversion coefficients $x_{(Ram)}$ are obtained from relation between integrated intensities of $A_{1g}(1)$ and $A_{1g}(2)$ modes in Raman spectra (Fig. 2)

Sample	a [Å] ±0.0004	u ±0.0003	x (r_o=1.365Å)	$x_{(Ram)}$
US-CO	8.3407	0.2540	0.90±0.02	0.82±0.05
ME	8.3503	0.2545	0.80±0.02	0.73±0.05
CO	8.3619	0.2548	0.72±0.02	0.71±0.04
MW-HT	8.3732	0.2554	0.60±0.02	0.67±0.04
MC-CO	8.3825	0.2558	0.51±0.02	0.58±0.04

In *FullProf Suite* the standard deviations σ(a) and σ(u) are given in "sum"-file (and σ(u) in "out"-file, also). Since the Shannon radii have two safe digits, according to rules of the determination of errors in calculation, the estimated cation inversion error is ±0.02.

In the case of $CoFe_2O_4$, small nanoparticles have smaller lattice constants than bigger nanoparticles, or crystalline material [10, 14]. Because of the incomplete tetrahedra and octahedra, there is a local contraction of the crystal lattice and the average oxygen radius is smaller than in the bulk. In this case it is estimated r_0 =1.36(5) Å. (With a Shannon's value of 1.38 Å, as for crystalline material, x would be >1.) It can be seen that as the lattice constant increases, the value of the inversion coefficient decreases.

3.2. Raman and Far-infrared spectroscopic analysis

Factor group analysis for $Fd\bar{3}m$ space group predicts 42 phonon modes for the normal cubic spinel structure: 3 acoustic of F_{1u} symmetry and 39 optic modes that are distributed among the following symmetries at the Brillouin zone centre [15, 16]:

$$\Gamma = A_{1g}(R) + E_g(R) + 3F_{2g}(R) + 4F_{1u}(IR) + F_{1g} + 2A_{2u} + 2E_u + 2F_{2u}$$

Five of these phonon modes are Raman active, namely A_{1g}, E_g and $3F_{2g}$; four are IR active, $4F_{1u}$, and remaining modes are silent.

All investigated $CoFe_2O_4$ samples showed a typical cubic spinel XRD pattern. Raman spectra are more sensitive to local symmetry and have asymmetric or dissociated peaks characteristic for inverse and partially inverse spinel structure of lower symmetry. For the sake of simplicity, Raman modes are assigned as in normal cubic spinel, Raman spectra are fitted with 7-8 Lorentzian peaks (Fig. 2).

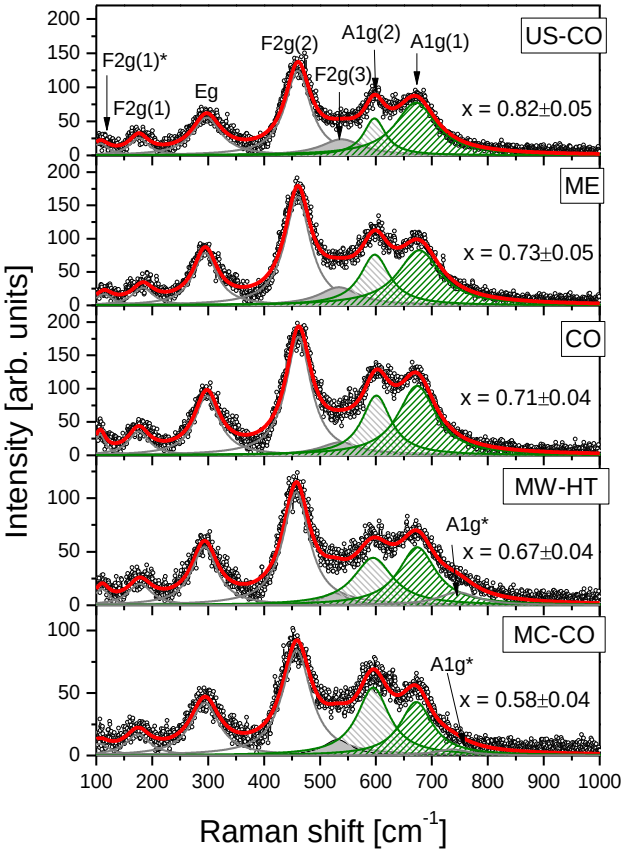

Fig. 2. Raman spectra $CoFe_2O_4$ ferrite prepared by various synthesis methods: US-CO ultrasonically assisted coprecipitation, ME - microemulsion method, CO - coprecipitation, MW-HT microwave assisted hydrothermal method and MC-CO coprecipitation followed by mechanochemical treatment (color online)

The values of mode wave numbers are generally in accordance with literature [17, 18]. Nano material obtained by micro-emulsion method - ME, with the biggest nanoparticles, has the highest wave number of A_{1g} (1) mode and US-CO obtained by ultrasonically assisted coprecipitation - the smallest.

A outstanding feature of the cobalt ferrite Raman spectra is the separation of the A_{1g} mode in two distinct parts: $A_{1g}(1)$ corresponds to the symmetric stretching of Fe^{3+} - O bonds in tetrahedrons and $A_{1g}(2)$ to the stretching of Co^{2+} - O bonds in tetrahedrons. Weak A_{1g}^{*} mode matches to the vibration of Fe^{3+} in incomplete tetrahedrons, as in maghemite. Due to the separation of Fe-O and Co-O oscillations, it is possible to estimate the degree of cation inversion (x), i.e. the Fe-content in the tetrahedral (A) site, as follows:

$$x = I_{A1g(1)} / [(I_{A1g(1)} + S \cdot I_{A1g(2)})]$$

where $I_{A1g(1,2)}$ are corresponding Lorentzian integrated areas and S = 0.59 - represents the relative oscillator strength of the Co^{2+}–O bonds with respect to the Fe^{3+}–O bonds in tetrahedrons. Oscillator strength is $k \propto Z_A Z_O / R_{tet}^3$ [19]. Estimated values of the coefficients of the inversion are given in Fig. 2 and Table 1. It is observed that the values of x obtained from Raman spectra, denoted in Table 1 as $x_{(Ram)}$, are in good agreement with the values obtained by XRD-structural analysis.

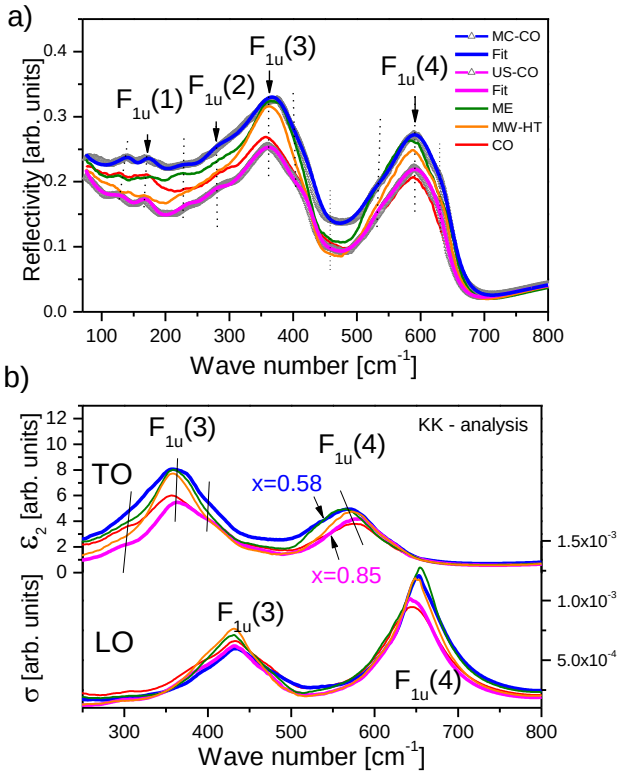

Fig. 3. Infrared reflectivity spectra of $CoFe_2O_4$ nanoparticles obtained by various synthesis procedures: a) Experimental spectra of eigenfrequencies from the centre of Brillouin zone recorded in far-IR and (partially) mid-IR range. Calculated spectra of two samples, MC-CO and US-CO are shown, also. b) Kramers-Krönig - analysis of spectra: imaginary part of complex dielectric constant, $\varepsilon_2(\omega) = Im(\varepsilon(\omega))$ and loss function, $\sigma(\omega) = - Im(1/\varepsilon(\omega))$ (see text) (color online)

The IR reflectivity spectra of $CoFe_2O_4$ nanoparticles obtained by various synthesis techniques are shown in Fig. 3a. In the range 700-800 cm^{-1} the FIR spectra were simulated (artificially extended) in order to perform the *Kramers-Krönig* analysis. It is clearly visible that spectra have more than four F_{1u} modes predicted by factor group analysis. All existing modes are indicated by dotted lines and the main modes are highlighted with arrows. Satellite peaks are noticeably weaker. In general, the number of vibration mode increases by canceling of degeneracy due to crystal lattice disordering, or the existence of defects and oxygen vacancies. The spectra are of relatively good intensity. The intensity roughly corresponds to the nanoparticle sizes of the tested samples. Stretching modes of cations in a dominantly tetrahedral and octahedral environment, $F_{1u}(4)$ and $F_{1u}(3)$, respectively, are the most pronounced. It is generally accepted that the low-frequency modes $F_{1u}(2)$ and $F_{1u}(1)$ originate from complex vibrations tetrahedral and octahedral groups following with significant displacement of cations. To analyze the spectra, we used *Kramers-Krönig* analysis [20-22], Fig. 3b, and also a Decoupled Plasmon – Phonon model of the complex dielectric function $\varepsilon(\omega)$ to simulate reflectivity spectra $R(\omega)$ [23, 24]. There is *a* noticeable increase in ω_{TO} of the dominantly tetrahedral mode $F_{1u}(4)$. with the increase of the inversion coefficient. It is expected due to an increase in the tetrahedral cation charge (more Fe^{3+} in tetrahedra) and decrease an effective cation radius what lead to increase of the vibration force constant and wave number. The wavenumbers of the other modes decrease slightly, indicating the dominant octahedral origin of these modes.

Magnetizations of cobalt ferrite samples obtained by various synthesis methods as the function of magnetic field are shown in Fig. 4.

In Fig. 4, the graphics of magnetization are given in order of ascending coercitive force, Hc. Coercitive force is connected with anisotropy energy, i.e. internal forces of the material, primarily magnetocrystalline energy. In the case of nanoferrites, magnetization for $H >> H$c can be describe by empirical relation ("the law of approach to saturation") consistent with Braun theory [25]:

$$M(\mathrm{H}) = M_s(0) \cdot \left(1 - \frac{B}{\mathrm{H}^2} + \cdots\right) + \chi_p \cdot H$$

Coefficient B is related to effective anisotropy constant as:

$$B = \frac{4 \cdot K_{eff}^2}{15 \cdot \mu_0^2 \cdot M_s^2}$$

For randomly oriented spherical polycrystalline nanomaterials with cubic symmetry, the magneto crystalline anisotropy is dominant and the effective anisotropy constant will be approximately equal to the principal anisotropy constant K_1 [26, 27]:

$$K_{eff} = K_1 = \mu_o \cdot M_s \cdot \sqrt{\frac{105 \cdot B}{8}}$$

So, via the coefficient *B*, determined by fitting the magnetization curve $M = M(H)$ for $H>>Hc$ by "the law of approach" (the fits - green solid lines - and corresponding formulas with best parameters are given in Fig. 4), the values of the coefficients of anisotropy K_1 are estimated for all $CoFe_2O_4$ samples. On the graphic given in Fig. 4, green circles, it can be seen that K_1 increases uniformly with the size of nanoparticles in the investigated samples.

The achieved saturation magnetization values for nano particle $CoFe_2O_4$ samples with particles of sizes 15.8-17.34 nm decrease linearly with the increase of the inversion coefficient. Sample ME, obtained by microemulsion method, with slightly larger nanoparticles (and a smaller number of surface defects) has a noticeably higher *M*s.

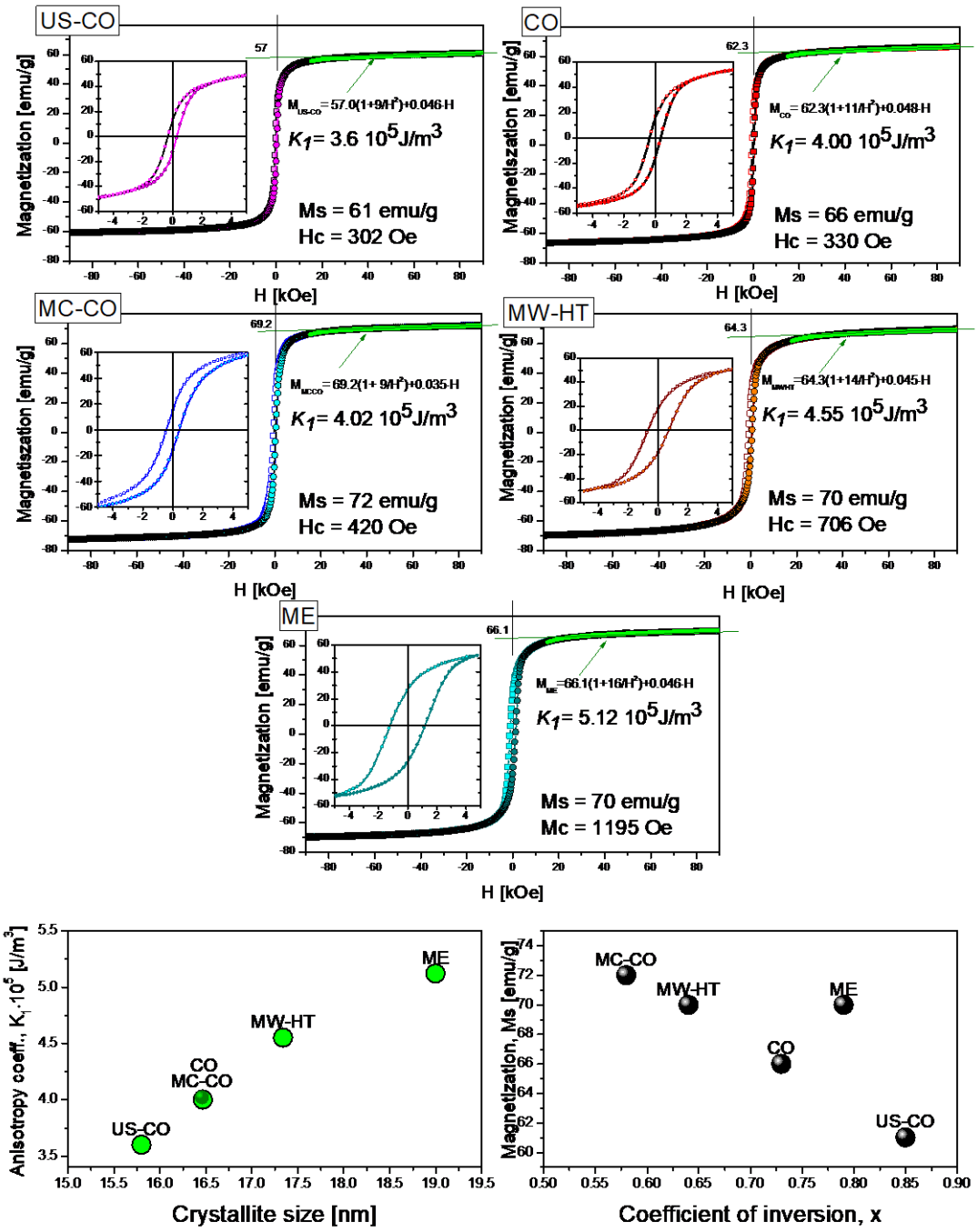

Fig. 4. Magnetic measurements of cobalt ferrite nanomaterials obtained by various synthesis methods: US-CO ultrasonically assisted coprecipitation, CO - coprecipitation, MC-CO coprecipitation followed by mechanochemical treatment, MW-HT microwave assisted hydrothermal method and ME microemulsion method. In each graphic for a certain sample is magnetization as the function of the magnetic field in the range ±90 kOe with the hysteresis loop in insert. Green solid lines are fits of magnetization for H>>Hc by "the law of approach" to saturation. In the bottom of the whole figure are presented - by green circles the dependence of the anisotropy coefficient, K_1 (obtained from "the law of approach") on the crystallite size and the saturation magnetization, Ms (black circles), as the function of the coefficient of the inversion, x, obtained by XRD structural analysis (color online)

The magnetizations of predominantly inverse ferrites with collinear and antiparallel magnetic moments in the tetrahedral (A) and octahedral (B) sublattice can be represented by Neel's formula:

$$Ms = M^B - M^A = \\ = [(2-x)\cdot\mu_{Fe} + x\cdot\mu_{Co}]^B - [(1-x)\cdot\mu_{Co} + x\cdot\mu_{Fe}]^A$$

where μ_{Fe} and μ_{Co} are magnetic moments of Fe and Co cations, respectively, expressed by the number of Bohr magnetons ($\mu_B = 9.27\cdot10\text{-}24$ J T^{-1}).

Based on the measured values of magnetization M_s and the values of x from XRD analysis, it can be estimated that the average magnetic moments at 300 K are: $\mu_{Fe} = 3.6\mu_B$ and $\mu_{Co} = 2.5\mu_B$.

A superparamagnetic component is present in each of our nanopowder samples. Except superparamagnetic particles, the surface layer of nanoparticles (with a disordered crystal structure - a large number of defects and oxygen vacancies) is decisively responsible for the reduced magnetization of nanoparticles compared to the bulk.

4. Conclusion

Single phase cobalt ferrite $CoFe_2O_4$ with nanoparticles of similar sizes (15.7-19 nm) was obtained by different synthesis methods: coprecipitation, ultrasonically assisted coprecipitation, coprecipitation followed by mechanochemical treatment, microemulsion and microwave assisted hydrothermal synthesis. Nanoparticles with different internal stresses and defects, different widths of nanoparticle size distribution, and above all - different cation inversion coefficients were obtained by the aforementioned synthesis methods. XRD analysis and spectroscopic methods Raman and FIR reflectivity confirm the quality of the obtained samples. Based on the Raman spectra of $CoFe_2O_4$ nanomaterials, with the characteristic, fully split A_{1g} mode into components corresponding to the vibrations of different cations in the tetrahedra, the inversion coefficient of the nanomaterials can be easily estimated. The cation inversion coefficients obtained by comparing the integrated areas of the components of A_{1g} Raman modes are in good agreement with the results obtained by XRD analysis. Measurement of magnetization as a function of magnetic field strength showed that $CoFe_2O_4$ nanoparticles have relatively high H_c values and K_1 anisotropy coefficient values that are almost an order of magnitude higher than in other ferrites. The value of K_1 directly depends on the size of the nanoparticles. The magnitude of the magnetization depends significantly on the inversion coefficient. In the case of larger nanoparticles (ME - 19 nm), the increase in magnetization, in addition to the decrease in the inversion coefficient, is largely influenced by a more regular crystal structure. Based on this investigation, it is obvious that in addition to the size of the nanoparticles, the method of obtaining them has a significant impact on the properties of nanomaterial. With small adjustments in the synthesis method, $CoFe_2O_4$ nanoparticles with properties desirable for various technical applications can be obtained.

Acknowledgment

The authors acknowledge funding provided by the Institute of Physics Belgrade and Faculty of Technology and Metallurgy Belgrade, through the financial support of the Ministry of Education, Science, and Technological Development of the Republic of Serbia. This research was supported by the Science Fund of the Republic of Serbia, Grant No. 7504386, Nano object in own matrix – Self composite – NOOM-SeC.

This paper is dedicated to the memory of our friend and colleague, Jelena Trajić.

References

[1] S. S. Desai, S. E. Shirsath, K. M. Batoo, S. F. Adil, M. Khan, S. M. Patange, Physica B: Physics of Condensed Matter. **596**, 412400 (2020).

[2] S. E. Shirsath, D. Wang, S. S. Jadhav, M. L. Mane, S. Li, Ferrites obtained by sol-gel method, in: L. Klein, M. Aparicio, A. Jitianu (Eds.), Handbook of Sol-Gel Science and Technology, Springer, Cham 695 (2018).

[3] Y. Kim, D. Kim, C. S. Lee, Physica B **337**, 42 (2003).

[4] V. H. Ojha, K. M. Kant, Physica B: Physics of Condensed Matter. **567**, 87 (2019).

[5] L. E. Caldeira, C. S. Erhardt, F. R. Mariosi, J. Venturini, R. Y. S. Zampiva, O. R. K. Montedo, S. Arcaro, C. P. Bergmann, S. R. Bragança, J. Magn. Magn. Mater. **550**, 169128 (2022).

[6] B. Abraime, K. El Maalam, L. Fkhar, A. Mahmoud, F. Boschini, M. Ait Tamerd, A. Benyoussef, M. Hamedoun, E. K. Hlil, M. Ait Ali, A. El Kenz, O. Mounkachi, J. Magn. Magn. Mater. **500**, 166416 (2020).

[7] M. Šuljagić, P. Vulić, D. Jeremić, V. Pavlović, S. Filipović, L. Kilanski, S. Lewinska, A. Slawska-Waniewska, M. R. Milenković, A. S. Nikolić, Lj. Andjelković, Mater. Res. Bull. **134**, 111117 (2021).

[8] J. Rodriguez-Carvajal, T. Roisnel, FullProf.98 and WinPLOTR: New Windows 95/NT Applications for Diffraction Commission for Powder Diffraction, International Union for Crystallography, Newletter, 20 (1998).

[9] R. V. Minin, V. I. Itin, V. A. Zhuravlev, V. A. Svetlichnyi, J. Physics: Conf. Series **1115**, 042011 (2018).

[10] R. S. Yadav, I. Kuřitka, J. Vilcakova, J. Havlica, J. Masilko, L. Kalina, J. Tkacz, J. Švec, V. Enev, M. Hajdúchová, Adv. Nat. Sci.: Nanosci. Nanotechnol. **8**, 045002 (2017).

[11] L. Lutterotti, S. Matthies, H.-R. Wenk, IUCr: Newsletter of the CPD **21**, 14 (1999).

[12] K. E. Sickafus, J. M. Wills, N. W. Grimes, J. Am.

Ceram. Soc. **82**(12), 3279 (1999).
[13] R. D. Shannon, Acta Cryst. **A32**, 751 (1976).
[14] A. López - Ortega, E. Lottini, C. de Julián Fernández, C. Sangregorio, Chem. Mater. **27**, 4048 (2015).
[15] G. A. de Wijs, C. M. Fang, G. Kresse, G. de With, Phys. Rev. B **65**, 094305 (2002).
[16] P. Thibaudeau, F. Gervais, J. Phys.: Condens. Matter. **14**, 3543 (2002).
[17] S. M. Ansari, K. C. Ghosh, R. S. Devan, D. Sen, P. U. Sastry, Y. D. Kolekar, C. V. Ramana, ACS Omega **5**, 19315 (2020).
[18] V. Bartunek, D. Sedmidubský, Š. Huber, M. Švecová, P. Ulbrich, O. Jankovský, Materials **11**, 1241 (2018).
[19] M. N. Iliev, D. Mazumdar, J. X. Ma, A. Gupta, F. Rigato, J. Fontcuberta, Phys. Rev. B **83**, 014108 (2011).
[20] A. B. Kuzmenko, Review of Scientific Instruments **76** (8), 083108 (2005).
[21] F. C. Jahoda, Phys. Rev. **107**, 1261 (1957).
[22] H. R. Phillip, E. A. Taft, Phys. Rev. **136**, A1445 (1964).
[23] F. Gervais, B. Piriou, Phys. Rev. B **10**, 1642 (1974).
[24] F. Gervais, Mater. Sci. Eng. **R 39**, 29 (2002).
[25] W. F. Brown, Jr, Phys. Rev. **58**, 736 (1940).
[26] J. F. Herbst, F. E. Pinkerton, Phys. Rev. B **57**, 10733 (1998).
[27] H. Jalili, B. Aslibeiki, A. G. Varzaneh, V. A. Chernenko, Beilstein J. Nanotechnol. **10**, 1348 (2019).

*Corresponding author: lzorica@yahoo.com